

CDMT-EHR: A Continuous-Time Diffusion Framework for Generating Mixed-Type Time-Series Electronic Health Records

Shaonan Liu, Yuichiro Iwashita, Soichiro Nakako, Masakazu Iwamura, *Senior Member, IEEE*, and Koichi Kise, *Member, IEEE*

Abstract—Electronic health records (EHRs) are invaluable for clinical research, yet privacy concerns severely restrict data sharing. Synthetic data generation offers a promising solution, but EHRs present unique challenges: they contain both numerical and categorical features that evolve over time. While diffusion models have demonstrated strong performance in EHR synthesis, existing approaches predominantly rely on discrete-time formulations, which suffer from finite-step approximation errors and coupled training-sampling step counts. We propose a continuous-time diffusion framework for generating mixed-type time-series EHRs with three contributions: (1) continuous-time diffusion with a bidirectional gated recurrent unit backbone for capturing temporal dependencies, (2) unified Gaussian diffusion via learnable continuous embeddings for categorical variables, enabling joint cross-feature modeling, and (3) a factorized learnable noise schedule that adapts to per-feature-per-timestep learning difficulties. Experiments on two large-scale intensive care unit datasets demonstrate that our method outperforms existing approaches in downstream task performance, distribution fidelity, and discriminability, while requiring only 50 sampling steps compared to 1,000 for baseline methods. Classifier-free guidance further enables effective conditional generation for class-imbalanced clinical scenarios.

Index Terms—Continuous-time diffusion, electronic health records, synthetic data.

I. INTRODUCTION

ELECTRONIC health records (EHRs) contain a wealth of clinical information, including vital signs and laboratory measurements, and play a critical role in clinical

This research was supported in part by JST ASPIRE (JPMJAP2403), and JSPS Grant-in-Aid for Challenging Research (Exploratory) (24K22339). Code will be made available upon acceptance. (Corresponding author: Yuichiro Iwashita.)

Shaonan Liu, Masakazu Iwamura, and Koichi Kise are with the Department of Core Informatics, Graduate School of Informatics, Osaka Metropolitan University, Sakai, Osaka 599-8531, Japan (e-mail: sc24697f@st.omu.ac.jp; masa.i@omu.ac.jp; kise@omu.ac.jp).

Yuichiro Iwashita is with the Smart Data & Knowledge Services Department, German Research Center for Artificial Intelligence (DFKI GmbH), 67663 Kaiserslautern, Germany, and the Department of Computer Science, RPTU University Kaiserslautern-Landau, 67663 Kaiserslautern, Germany (e-mail: yuichiro.iwashita@dfki.de).

Soichiro Nakako is with the Department of Hematology and Department of Laboratory Medicine and Medical Informatics, Graduate School of Medicine, Osaka Metropolitan University, Osaka 545-8585, Japan (e-mail: s-nakako@omu.ac.jp).

research. With advances in machine learning, EHRs have been increasingly applied to downstream tasks such as disease diagnosis and in-hospital mortality prediction, underscoring their growing importance [1]. However, the sensitive personal information embedded in EHRs significantly restricts data access and sharing, which hinders the development of machine learning models for healthcare applications.

Several approaches have been proposed to address this challenge, but each has limitations. Anonymization techniques such as data masking have been widely adopted, yet re-identification risks remain high [2], and such processing can distort the statistical properties of the original data.

Against this background, generating synthetic data that preserves the statistical characteristics of real EHRs has emerged as a promising alternative. EHR synthesis must simultaneously address two key challenges. (1) EHRs contain a mixture of numerical variables (e.g., body temperature and blood pressure) and categorical variables (e.g., diagnostic codes and medication flags), which requires a unified framework to model heterogeneous data types. (2) EHRs are time-series data in which patient states evolve over time, which necessitates models that capture temporal dependencies. Various generative models have been proposed, including rule-based [3], [4], variational auto-encoder (VAE)-based [5], [6], and generative adversarial network (GAN)-based [7]–[11] methods. However, these approaches have not adequately addressed both challenges simultaneously.

Recently, diffusion models [12], [13], which have demonstrated superior performance in image generation, have attracted attention for EHR synthesis. Diffusion models generate high-quality data by progressively adding noise in a forward diffusion process and then learning to reverse this process through a denoising model. Several diffusion-based EHR generation methods have been proposed [14]–[20]. However, most focus on either a single variable type or non-temporal data, leaving the mixed-type time-series challenge largely unaddressed. TimeDiff [21], which uses a bidirectional RNN-based discrete-time diffusion model for mixed-type temporal EHRs, represents a notable exception. Nevertheless, TimeDiff and most other diffusion-based EHR methods rely on denoising diffusion probabilistic models (DDPMs), which have the following inherent limitations [13]. (1) The forward process is approximated by finite discrete steps, which introduces

approximation errors. (2) The sampling step count is coupled with the training step count, which degrades sampling efficiency. (3) A fixed noise schedule shared across all features cannot adapt to the heterogeneous marginal distributions present in EHRs.

Continuous-time diffusion models [13] address the first two limitations by formulating the diffusion process using stochastic differential equations (SDEs), which decouple training and sampling step counts. For mixed-type static tabular data, continuous-time diffusion frameworks such as TabDiff [22] and the continuous diffusion model for mixed-type tabular data (CDTD) [23] have demonstrated state-of-the-art performance. TabDiff addresses the schedule limitation through learnable per-feature noise schedules and employs separate diffusion processes for numerical (Gaussian) and categorical (mask diffusion) features, while CDTD maps categorical variables into a continuous embedding space to apply unified Gaussian diffusion. However, neither framework supports time-series data, leaving a gap for temporal EHR generation.

In this work, we propose CDMT-EHR, a continuous-time diffusion framework for mixed-type time-series EHR generation by extending TabDiff with the following three contributions:

- 1) **Continuous-time diffusion for temporal EHR generation:** We introduce continuous-time diffusion to mixed-type time-series EHR generation by incorporating a bidirectional gated recurrent unit (BiGRU) [24] as the denoising backbone. This enables flexible sampling with decoupled training and sampling step counts while capturing temporal dependencies through the hidden states of the BiGRU.
- 2) **Unified Gaussian diffusion via continuous embeddings:** Following CDTD [23], we map categorical variables into a learnable continuous embedding space and apply the same Gaussian diffusion process as for numerical variables. This unified continuous-space diffusion enables more effective joint modeling of cross-feature dependencies compared to combining separate Gaussian and mask diffusion processes.
- 3) **Factorized learnable noise schedule:** We propose a factorized learnable noise schedule that decomposes each feature-timestep pair into global, feature-specific, and time-specific components. This extends TabDiff’s per-feature schedule to the temporal setting while reducing the number of learnable parameters from $O(F \times L)$ to $O(F + L)$, where F is the number of features and L is the sequence length, adapting to per-feature-per-timestep learning difficulties.

We evaluate our method on two large-scale intensive care unit (ICU) datasets, including MIMIC-III [25]–[27] and eICU [28], across three perspectives, namely downstream task performance, fidelity, and discriminability. Our method consistently outperforms the existing TimeDiff baseline while requiring only 50 sampling steps compared to 1,000 steps for TimeDiff. Furthermore, we demonstrate that classifier-free guidance (CFG) enables effective conditional generation for data augmentation in class-imbalanced clinical scenarios.

II. RELATED WORK

A. Non-Diffusion EHR Generation Models

Early approaches to synthetic EHR generation include rule-based methods [3], [4], which generate data according to predefined clinical rules but produce limited diversity. With the development of deep generative models, VAE-based methods [5], [6] offer stable training but often yield lower-quality samples, while GAN-based methods [7]–[11] can produce high-quality data but suffer from mode collapse and training instability [17]. Furthermore, most existing studies target simplified data structures, e.g., only diagnostic codes, that do not fully reflect the complexity of real-world EHRs.

B. Diffusion-Based EHR Generation Models

Diffusion models have been increasingly applied to EHR generation [14]–[20], [29], [30], demonstrating improvements in both data quality and privacy over conventional generative models. However, most of these methods are limited to a single variable type or non-temporal data. TimeDiff [21] addresses this gap by applying a DDPM-based diffusion model with a bidirectional RNN backbone to mixed-type temporal EHRs. While TimeDiff achieves competitive performance, it inherits the limitations of discrete-time diffusion, including finite-step approximation errors, coupled training-sampling step counts, and a fixed noise schedule that cannot adapt to heterogeneous feature distributions.

C. Continuous-Time Diffusion for Mixed-Type Data

To overcome the limitations of discrete-time diffusion, TabDiff [22] proposes continuous-time diffusion frameworks for mixed-type static tabular data. TabDiff uses Gaussian diffusion for numerical features and mask diffusion [31] for categorical features, with learnable per-feature noise schedules. However, mask diffusion constrains categorical representations to either a fixed category or a mask state, which prevents smooth inter-category transitions and potentially limits generation quality for temporal data where categories may evolve over time.

CDTD [23] addresses this by mapping categorical variables into a continuous embedding space and applying unified Gaussian diffusion across all features. This enables joint modeling of cross-feature dependencies in a shared continuous space. However, CDTD applies a common learnable noise schedule per variable type rather than per individual feature, which may not optimally adapt to features with diverse marginal distributions within the same type.

Critically, both TabDiff and CDTD are designed for static (non-temporal) tabular data. Our work extends TabDiff to temporal sequences while incorporating the continuous embedding approach of CDTD and introducing a factorized per-feature-per-timestep noise schedule.

III. PROPOSED METHOD

We propose a continuous-time diffusion framework for mixed-type time-series EHR generation that extends TabDiff [22] through three key modifications: (1) a temporal extension using a BiGRU backbone for efficient temporal

modeling with label information propagation, (2) unified Gaussian diffusion via continuous embeddings for categorical variables, and (3) factorized learnable noise schedules. Fig. 1 presents an overview of the proposed method. In the following subsections, we first introduce the necessary preliminaries from TabDiff, then describe each contribution in detail.

A. Preliminaries: TabDiff

TabDiff [22] is a continuous-time diffusion model for mixed-type static tabular data. An individual data sample x is represented as the concatenation of numerical and categorical features: $x = [x^{\text{num}}, x^{\text{cat}}]$, where $x^{\text{num}} \in \mathbb{R}^{M_{\text{num}}}$ denotes M_{num} -dimensional numerical features and x^{cat} denotes M_{cat} categorical features, with the j -th categorical feature represented as a one-hot vector $(x^{\text{cat}})_j \in \{0, 1\}^{C_j+1}$, where C_j is the number of categories and the additional dimension represents a special mask state.

TabDiff formulates the diffusion process in continuous time $t \in [0, 1]$, where $t = 0$ corresponds to clean data and $t = 1$ to pure noise. For numerical features, a variance-exploding SDE [13], [32] defines the forward process:

$$x_t^{\text{num}} = x_0^{\text{num}} + \sigma^{\text{num}}(t) \epsilon, \quad \epsilon \sim \mathcal{N}(0, I_{M_{\text{num}}}) \quad (1)$$

where $\sigma^{\text{num}}(t)$ is the noise schedule for numerical features. The corresponding reverse process is given by an ordinary differential equation (ODE):

$$dx^{\text{num}} = - \left[\frac{d}{dt} \sigma^{\text{num}}(t) \right] \sigma^{\text{num}}(t) \nabla_x \log p_t(x^{\text{num}}) dt \quad (2)$$

TabDiff introduces learnable per-feature noise schedules using a power-mean parameterization. For the i -th numerical feature:

$$\sigma_{\rho_i}^{\text{num}}(t) = (\sigma_{\min}^{1/\rho_i} + t(\sigma_{\max}^{1/\rho_i} - \sigma_{\min}^{1/\rho_i}))^{\rho_i} \quad (3)$$

where ρ_i is a learnable parameter for the i -th feature, and σ_{\min} and σ_{\max} are fixed hyperparameters that anchor the noise range.

For categorical features, TabDiff uses mask diffusion [31], which progressively transitions categories to a special mask state. However, as discussed in Section II, this approach has limitations for temporal data.

A denoising model f_θ , which approximates the score function $\nabla_x \log p_t(x)$ in (2), is jointly trained on both feature types, and TabDiff’s total loss combines a noise prediction loss for numerical features and a masked cross-entropy loss for categorical features.

B. Temporal Extension with BiGRU

TabDiff processes each data sample as a single row of a table with shape $[N, F]$, where N is the number of samples and F is the number of features. Real-world EHRs, however, are time-series with shape $[N, F, L]$, where L is the number of time steps. Directly extending TabDiff’s Transformer backbone to the temporal dimension would incur prohibitive attention complexity, and Transformer-based alternatives such as TimeSformer [33] limit label information propagation across

features due to their separate temporal and spatial attention design.

We therefore adopt a BiGRU [24] as the denoising backbone, following TimeDiff [21]. At each time step, the BiGRU receives a feature vector concatenating all variables (including labels for conditional generation; see Section III-G), allowing label information to naturally propagate via hidden states with $O(F \cdot L)$ complexity.

Within the BiGRU backbone, we apply layer normalization followed by feature-wise linear modulation for diffusion time conditioning:

$$h_{\text{out}} = h_{\text{in}} \cdot (1 + \gamma(t)) + \omega(t) \quad (4)$$

where h_{in} and h_{out} are the input and output latent representations within the BiGRU, and $\gamma(t)$ and $\omega(t)$ are scale and shift parameters learned from the embedding of the diffusion time step t . This enables the model to adapt its behavior across different noise levels.

C. Unified Gaussian Diffusion via Continuous Embeddings

As discussed in Sections II and III-A, TabDiff’s mask diffusion for categorical features prevents smooth intermediate representations and hinders unified cross-feature modeling. To address these limitations, we adopt the continuous embedding approach of CDTD [23]. For the j -th categorical feature with C_j categories, each category $k \in \{0, 1, \dots, C_j-1\}$ is assigned a learnable d -dimensional embedding vector $e_{j,k} \in \mathbb{R}^d$. The embedding is L2-normalized and scaled:

$$x^{\text{emb}} = \frac{e_{j,k}}{\|e_{j,k}\|_2} \cdot \sqrt{d} \quad (5)$$

The same Gaussian forward process (1) and reverse ODE (2) are then applied to these continuous embeddings, with a separate noise schedule $\sigma^{\text{emb}}(t)$.

By applying unified Gaussian diffusion to both numerical features and categorical embeddings, all features diffuse in a shared continuous space. This enables the model to jointly learn dependencies between numerical and categorical features more effectively than when separate diffusion processes are used.

D. Factorized Learnable Noise Schedules

EHR features exhibit heterogeneous marginal distributions; body temperature and blood pressure, for instance, have very different statistical characteristics, and the properties of each feature may also vary across time steps due to missing data patterns and temporal dynamics. This heterogeneity leads to uneven learning difficulty across features and time steps.

A naive approach of assigning an independent ρ parameter to each feature-timestep pair would require $O(F \times L)$ parameters, raising scalability and overfitting concerns. Instead, we propose a factorized parameterization that decomposes ρ into additive components:

$$\rho_{f,l} = \rho_{\text{global}} + \rho_{\text{feature}}[f] + \rho_{\text{time}}[l] \quad (6)$$

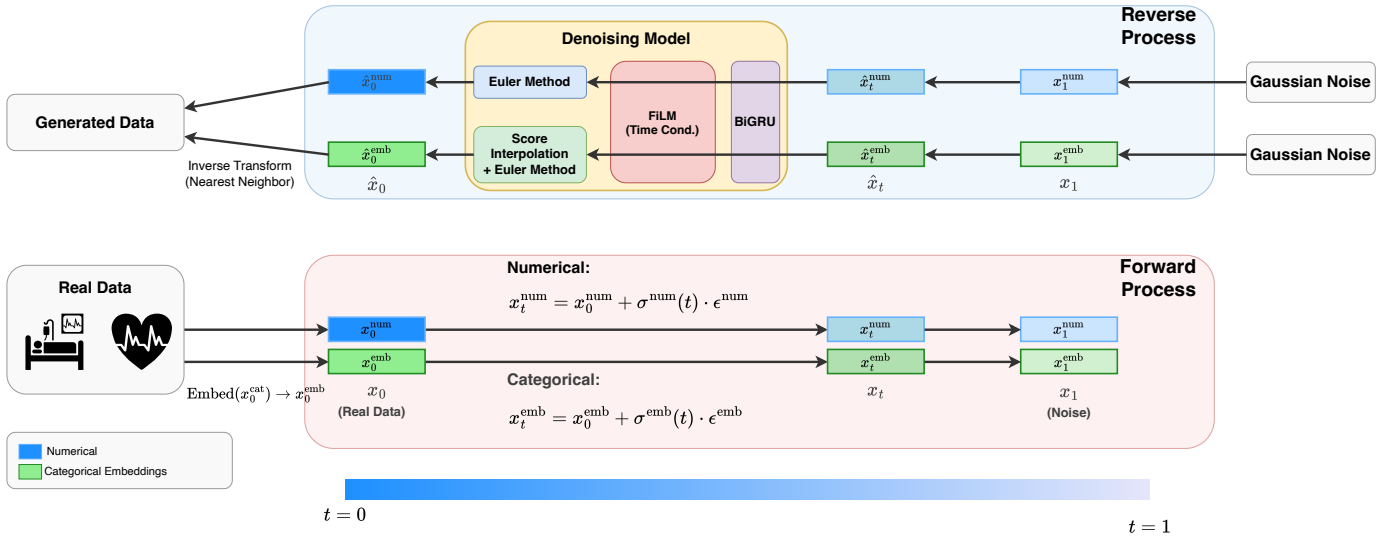


Fig. 1. Overview of the proposed method. Categorical variables are mapped into a learnable continuous embedding space, and both numerical and categorical (embedded) features undergo unified Gaussian diffusion. A BiGRU backbone captures temporal dependencies. Factorized learnable noise schedules adapt to per-feature-per-timestep learning difficulties.

where ρ_{global} is a scalar shared across all features and time steps, $\rho_{\text{feature}}[f]$ is an adjustment for feature f , and $\rho_{\text{time}}[l]$ is an adjustment for time step l . Both ρ_{feature} and ρ_{time} are initialized to zero, so that learning proceeds from the global baseline. This $\rho_{f,l}$ is substituted into (3) in place of ρ_i , yielding per-feature-per-timestep noise schedules with only $O(F + L)$ parameters.

Since categorical features now undergo Gaussian diffusion in the continuous embedding space (Section III-C), the same power-mean schedule can be applied to both feature types. We apply separate power-mean schedules for numerical and categorical (embedded) features, each with its own set of factorized parameters. This allows different σ_{max} values for each type: we use $\sigma_{\text{max}}^{\text{num}} = 80$ for numerical features and $\sigma_{\text{max}}^{\text{emb}} = 100$ for categorical embeddings, following CDTD [23]. The larger σ_{max} for embeddings accounts for the fact that the L2-normalized embeddings have norm \sqrt{d} after (5), requiring a greater noise scale for full diffusion.

E. Loss Function

The change in categorical diffusion from mask-based to Gaussian embedding-based necessitates a corresponding change in the loss function. The categorical loss of TabDiff computes a masked cross-entropy only at positions in the mask state, which is not applicable when mask states do not exist.

1) **Numerical loss:** For numerical features, we adopt a data-prediction formulation based on EDM [32], where the denoising model directly predicts the clean data \hat{x}_0^{num} rather than the noise ϵ . Data prediction is mathematically equivalent to noise prediction [32] but is more naturally aligned with the categorical loss design, where the model predicts category probabilities from noisy embeddings. The numerical loss applies a noise-level-dependent weight $\lambda(\sigma)$, where $\sigma = \sigma^{\text{num}}(t)$, for training stability:

$$\mathcal{L}_{\text{num}}(\theta, \rho) = \mathbb{E}_{x_0, t, \epsilon} [\lambda(\sigma) \cdot \|\hat{x}_0^{\text{num}} - x_0^{\text{num}}\|_2^2] \quad (7)$$

2) **Categorical loss:** For categorical features, following CDTD [23], we use a cross-entropy loss between the model's predicted category probabilities and the ground-truth categories. Unlike the mask diffusion loss, this loss is computed at *all* positions:

$$\mathcal{L}_{\text{emb}}(\theta, \rho) = \mathbb{E}_{x_0, t, \epsilon} \left[-\frac{1}{M_{\text{cat}} L} \sum_{j, l} \log p_{\theta}(x_0^{\text{cat}, (l, j)} | x_t^{\text{emb}}, t) \right] \quad (8)$$

where $x_0^{\text{cat}, (l, j)}$ is the ground-truth category of the j -th categorical feature at time step l , and $p_{\theta}(\cdot | x_t^{\text{emb}}, t)$ is the category probability computed via softmax from the model's logit output.

3) **Total loss:** The two losses are combined with weighting coefficients λ_{num} and λ_{emb} :

$$\mathcal{L}(\theta, \rho) = \lambda_{\text{num}} \mathcal{L}_{\text{num}}(\theta, \rho) + \lambda_{\text{emb}} \mathcal{L}_{\text{emb}}(\theta, \rho) \quad (9)$$

F. Training and Sampling

The training and sampling procedures are summarized in Algorithms 1 and 2 in the supplementary material.

During training, the denoising model uses the EDM [32] preconditioning framework to normalize input and output scales across noise levels.

During sampling, the reverse ODE (2) is solved numerically using the Euler method. For numerical features, the score function is approximated as $\nabla_x \log p_t(x^{\text{num}}) \approx (x_t^{\text{num}} - \hat{x}_0^{\text{num}}) / (\sigma^{\text{num}}(t))^2$ and substituted into (2) to derive the Euler update. For categorical features, the denoised embedding estimate \hat{x}_0^{emb} is computed via score interpolation [23]:

$$\hat{x}_0^{\text{emb}} = \mathbb{E}[x_0^{\text{emb}} | x_t] = \sum_{k=0}^{C_j-1} p_{\theta}(k | x_t) \cdot e_{j, k} \quad (10)$$

where $p_{\theta}(k | x_t) = \text{softmax}(\text{logits}_j)_k$. This estimate is then used in an Euler update analogous to that for numerical

TABLE I
DATASET SPECIFICATIONS

	MIMIC-III	eICU
Training samples	20,920	48,849
Validation samples	5,230	16,269
Numerical features	7	4
Categorical features	7	4
Sequence length	25	272
Time interval	1 hour	5 minutes

features. After sampling is complete, the final embeddings x_0^{emb} are converted to categorical indices via nearest-neighbor lookup.

G. Classifier-Free Guidance for Conditional Generation

We incorporate CFG [34] to support conditional generation, which is particularly valuable for EHR data where important clinical events (e.g., in-hospital mortality) are rare, resulting in imbalanced label distributions. CFG enables generating EHRs conditioned on a target label y , facilitating data augmentation for underrepresented classes.

During training, the label information y is replaced with a zero vector with probability p_{drop} , enabling the model to learn both conditional and unconditional predictions. During sampling, conditional and unconditional predictions are interpolated:

$$\tilde{x}_0^{\text{num}} = (1 + w_{\text{num}}) \hat{x}_{0,c}^{\text{num}} - w_{\text{num}} \hat{x}_{0,u}^{\text{num}} \quad (11)$$

$$\widetilde{\text{logits}} = (1 + w_{\text{cat}}) \text{logits}_c - w_{\text{cat}} \text{logits}_u \quad (12)$$

where $\hat{x}_{0,c}^{\text{num}}$ and logits_c are conditional predictions (with label y), $\hat{x}_{0,u}^{\text{num}}$ and logits_u are unconditional predictions (with y replaced by \emptyset), and w_{num} , w_{cat} are guidance strengths for numerical and categorical features, respectively.

IV. EXPERIMENTS

A. Datasets

We evaluate our method on two large-scale publicly available ICU datasets. Table I summarizes the dataset specifications. Both datasets are de-identified and publicly available, with access granted through the respective data use agreements.

MIMIC-III [25]–[27]: Following the preprocessing of TimeDiff [21], we extract seven physiological variables (body temperature, systolic blood pressure, diastolic blood pressure, mean arterial pressure, heart rate, respiratory rate, and oxygen saturation) at 1-hour intervals from the first 24 hours of ICU admission. Missingness masks for each variable and an in-hospital mortality flag are appended as categorical features. Missing values are imputed hierarchically using last observation carried forward, per-patient mean, and dataset-wide mean, in that order.

eICU [28]: Similarly following TimeDiff’s preprocessing, we extract four physiological variables, namely heart rate, respiratory rate, oxygen saturation, and mean arterial pressure, at 5-minute intervals from the first 24 hours. Missingness masks and a mortality flag are appended. Only patients with continuously available observations are included.

B. Baselines

We primarily compare with TimeDiff [21], a DDPM-based diffusion model for mixed-type temporal EHRs, in two variants, namely **TimeDiff-GRU** (original BiGRU backbone) and **TimeDiff-Trans** (backbone replaced by a Transformer). For our method, we evaluate three generation modes, including **Ours uncond** (unconditional generation), **Ours CFG-comb** (conditional generation with CFG, combining samples according to the original label distribution), and **Ours CFG-bal** (conditional generation with balanced sampling across labels).

C. Evaluation Metrics

We evaluate synthetic data quality from three complementary perspectives:

1) **Downstream task performance**: We assess whether synthetic data can serve as a substitute for real data in training machine learning models. Binary classification models are trained on synthetic data and tested on held-out real data (train on synthetic, test on real (TSTR)). We use three classifiers, including bidirectional long short-term memory (LSTM), Transformer, and hybrid CNN-LSTM, and report the mean area under the receiver operating characteristic curve (AUC) across classifiers and five random seeds. The real-data baseline (train on real, test on real (TRTR)) serves as the upper bound.

2) **Fidelity**: We evaluate how well synthetic data preserves the statistical properties of real data. For numerical features, we compute maximum mean discrepancy (MMD) for distributional distance, correlation matrix mean absolute error (Corr MAE) for inter-feature dependency preservation, autocorrelation function mean squared error (ACF MSE) for temporal pattern preservation, and dynamic time warping (DTW) for time-series shape similarity. For categorical features, we compute total variation distance (TVD) for marginal distribution fidelity, and transition matrix distance (Trans Dist) for temporal transition pattern preservation.

3) **Discriminability**: The classifier two-sample test (C2ST) trains a binary classifier to discriminate real from synthetic data. We use three discriminators, including logistic regression, multi-layer perceptron (MLP), and LSTM, and report the mean AUC over five random seeds; values closer to 0.5 indicate less distinguishable synthetic data.

D. Implementation Details

Our model is trained using the Adam optimizer with a learning rate of 0.001 and a batch size of 4,096 for 8,000 epochs. Exponential moving average (EMA) with a decay rate of 0.997 is maintained for both model parameters and noise schedule parameters throughout training [32]. For sampling, we use the checkpoint with the lowest EMA-based loss and generate data using the first-order Euler method with 50 steps. EDM preconditioning parameters are set to $\sigma_{\text{min}} = 0.002$ and $\sigma_{\text{data}} = 0.5$, with $\sigma_{\text{max}}^{\text{num}} = 80$ for numerical features and $\sigma_{\text{max}}^{\text{emb}} = 100$ for categorical embeddings [23]. The BiGRU backbone consists of 3 layers with a hidden dimension of 64. The categorical embedding dimension is $d = 16$. The loss weights are set to $\lambda_{\text{num}} = \lambda_{\text{emb}} = 1.0$. The global noise

TABLE II
DOWNSTREAM TASK AUC (MEAN OF 3 CLASSIFIERS, \uparrow)

Model	MIMIC-III	eICU
TRTR	0.770 \pm 0.005	0.747 \pm 0.003
TimeDiff-GRU	0.663 \pm 0.008	0.607 \pm 0.010
TimeDiff-Trans	0.689 \pm 0.011	0.642 \pm 0.008
Ours uncond	0.729 \pm 0.006	0.708 \pm 0.004
Ours CFG-comb	0.743 \pm 0.004	0.688 \pm 0.005
Ours CFG-bal	0.751 \pm 0.006	0.689 \pm 0.006

schedule parameter is initialized to $\rho_{\text{global}} = 1.0$ for numerical features and $\rho_{\text{global}} = 7.0$ for categorical embeddings, with feature-specific and time-specific components initialized to zero. For classifier-free guidance, the label drop probability is $p_{\text{drop}} = 0.1$, and guidance weights are set to $w_{\text{num}} = w_{\text{cat}} = 2.0$.

For TimeDiff baselines, we use the original code¹ provided by the authors with default settings and 1,000 sampling steps [21]. All experiments are conducted on either a single NVIDIA TITAN RTX or a single NVIDIA RTX A6000 GPU.

E. Results

1) *Downstream task performance*: Table II presents the downstream task results using all features. Our method outperforms both TimeDiff variants on both datasets, approaching the real-data upper bound (TRTR) most closely. On MIMIC-III, Ours CFG-bal achieves the best mean AUC of 0.751, while Ours uncond achieves 0.708 on eICU. These results are achieved with only 50 sampling steps, compared to 1,000 steps for TimeDiff. Since both methods use a BiGRU backbone with comparable per-step cost, the continuous-time formulation with unified Gaussian diffusion enables substantially faster and higher-quality generation.

On MIMIC-III, CFG improves performance over unconditional generation, with CFG-bal outperforming CFG-comb. This is consistent with the role of balanced sampling in addressing the imbalanced label distribution (mortality rate $\approx 8\%$). On eICU, however, unconditional generation performs best. We attribute this to the much longer sequence length (272 vs. 25), which dilutes the relative importance of the label that is shared across all time steps.

2) *Fidelity*: Table III presents fidelity metrics for both numerical and categorical features. CFG-bal is excluded as it intentionally distorts the label distribution. Our method shows substantial improvements in most numerical metrics on both datasets. On eICU, Ours uncond achieves a 77% reduction in MMD (0.046 vs. 0.194–0.196), 63% reduction in Corr MAE, and 95% reduction in ACF MSE compared to both TimeDiff variants. On MIMIC-III, our method achieves the best Corr MAE and ACF MSE, with competitive MMD. For DTW, TimeDiff-GRU achieves the lowest values, as DTW measures pairwise shape similarity and is more sensitive to sample-level variation, suggesting that our method better preserves distributional properties at the population level.

For categorical features, TimeDiff-Trans achieves the lowest TVD on both datasets. CFG consistently improves both TVD and Trans Dist for our method. The continuous embedding approach prioritizes cross-feature relationships over exact marginal reproduction, which may explain the TVD gap while yielding substantially better downstream task performance (Table II).

3) *Discriminability*: Table IV presents C2ST results. Our method achieves AUC values substantially closer to 0.5 across all discriminators and datasets, indicating that the generated data is significantly harder to distinguish from real data.

For the simplest linear model (logistic regression), our method yields AUC close to 0.5, while TimeDiff baselines show higher AUC particularly on eICU (0.735 for GRU, 0.979 for Trans). With the MLP discriminator, TimeDiff-GRU achieves AUC above 0.96 on both datasets, indicating near-perfect discrimination, whereas our method remains around 0.59. With the LSTM discriminator, which captures temporal patterns, our method achieves the lowest AUC values (0.516 on MIMIC-III, 0.510 on eICU), suggesting that the continuous-time diffusion model effectively reproduces temporal statistical properties.

The remaining gap with the MLP discriminator (≈ 0.59) suggests room for improvement in capturing complex nonlinear inter-feature dependencies.

F. Ablation Studies

We conduct ablation studies on the MIMIC-III dataset to investigate the contribution of each component, using downstream task AUC as the primary metric.

1) *Categorical Variable Modeling: Mask vs. Embedding*: Table V compares two categorical variable modeling approaches: mask diffusion (Ours-Mask, as in the original TabDiff) and continuous embedding with Gaussian diffusion (Ours-Emb, our proposed approach). Ours-Emb outperforms Ours-Mask across all evaluation models and generation modes. The improvement is particularly pronounced with CFG, where Ours-Emb achieves an AUC of 0.751 (CFG-bal) compared to 0.678 for Ours-Mask. This confirms the effectiveness of unified Gaussian diffusion: because all features share the same continuous diffusion space, cross-feature dependencies are maintained during conditional generation, whereas mask diffusion processes categorical features independently from numerical features.

2) *Learnable vs. Fixed Noise Schedule*: Table VI compares the factorized learnable noise schedule (proposed) with a fixed schedule (where the shape parameter ρ is not learned and no temporal adaptation is applied). Both configurations share the same noise range ($\sigma_{\text{min}}, \sigma_{\text{max}}$) following EDM [32] and CDTD [23]; only the ρ parameter controlling the interpolation curve shape is learned.

As noted by Karras et al. [32], the noise range dominates generation quality in the continuous-time limit. However, with finite sampling steps (50 in our case), ρ determines the step allocation: $\rho > 1$ allocates more steps to low-noise regions, and $\rho < 1$ to high-noise regions. Learning ρ per feature and time step thus enables automatic adaptation of step allocation to each feature’s difficulty.

¹<https://github.com/MuhangTian/TimeDiff>

TABLE III
FIDELITY METRICS (\downarrow). BEST RESULTS PER DATASET ARE **BOLDED**.

Dataset	Method	Numerical				Categorical	
		MMD	Corr MAE	ACF MSE	DTW	TVD	Trans Dist
MIMIC-III	TimeDiff-GRU	0.0874	0.0237	0.00523	45.9	0.036	0.225
	TimeDiff-Trans	0.0373	0.0129	0.00477	48.8	0.002	0.008
	Ours uncond	0.0498	0.0100	0.00025	49.5	0.027	0.047
	Ours CFG-comb	0.0356	0.0270	0.00040	50.2	0.021	0.035
eICU	TimeDiff-GRU	0.1955	0.0365	0.00560	114.3	0.058	0.365
	TimeDiff-Trans	0.1941	0.0461	0.00311	168.5	0.012	0.099
	Ours uncond	0.0456	0.0136	0.00027	135.4	0.040	0.100
	Ours CFG-comb	0.0711	0.0564	0.00192	150.8	0.022	0.074

TABLE IV
DISCRIMINABILITY (C2ST) AUC (CLOSER TO 0.5 IS BETTER). BEST RESULTS PER DATASET ARE **BOLDED**.

Dataset	Method	Logistic	MLP	LSTM
MIMIC-III	TimeDiff-GRU	.575 \pm .005	.962 \pm .005	.951 \pm .006
	TimeDiff-Trans	.582 \pm .005	.885 \pm .020	.540 \pm .006
	Ours uncond	.536 \pm .004	.593 \pm .005	.516 \pm .004
	Ours CFG-comb	.554 \pm .002	.617 \pm .005	.526 \pm .005
eICU	TimeDiff-GRU	.735 \pm .003	.968 \pm .002	.916 \pm .011
	TimeDiff-Trans	.979 \pm .001	.988 \pm .001	.886 \pm .033
	Ours uncond	.530 \pm .005	.584 \pm .004	.510 \pm .004
	Ours CFG-comb	.568 \pm .007	.626 \pm .006	.570 \pm .003

TABLE V
ABLATION: MASK DIFFUSION VS. CONTINUOUS EMBEDDING
DOWNSTREAM TASK AUC (MEAN OF 3 CLASSIFIERS, \uparrow)

Mode	Ours-Mask	Ours-Emb
uncond	0.711 \pm 0.005	0.729 \pm 0.006
CFG-comb	0.671 \pm 0.007	0.743 \pm 0.004
CFG-bal	0.678 \pm 0.009	0.751 \pm 0.006

The learnable schedule improves downstream task performance (Table VI), with the largest gain in the unconditional setting (0.729 vs. 0.707). Fidelity metrics also favor the learnable schedule in most indicators, while C2ST results show marginal trade-offs (see the supplementary material for details).

3) *Data Augmentation with Real Data*: Table VII evaluates data augmentation on MIMIC-III. In the upper half, limited real data is supplemented with synthetic data to match the full dataset size (20,920 samples) using the T(S+R)TR framework. CFG-based augmentation with 50% real data achieves a mean AUC of 0.763, reaching 99.1% of the full real-data baseline (TRTR: 0.770). CFG outperforms unconditional generation

TABLE VI
ABLATION: LEARNABLE VS. FIXED NOISE SCHEDULE
DOWNSTREAM TASK AUC (MEAN OF 3 CLASSIFIERS, \uparrow)

Mode	Learnable	Fixed
uncond	0.729 \pm 0.006	0.707 \pm 0.009
CFG-comb	0.743 \pm 0.004	0.742 \pm 0.006
CFG-bal	0.751 \pm 0.006	0.745 \pm 0.006

TABLE VII
DATA AUGMENTATION ON MIMIC-III
DOWNSTREAM TASK AUC (MEAN OF 3 CLASSIFIERS, \uparrow)

Setting	uncond	CFG-comb
TRTR (100% Real)	0.770	
10% Real + 90% Synth	0.693 \pm 0.005	0.726 \pm 0.002
25% Real + 75% Synth	0.681 \pm 0.010	0.734 \pm 0.003
50% Real + 50% Synth	0.753 \pm 0.005	0.763 \pm 0.003
100% Real + 100% Synth	0.775 \pm 0.005	0.768 \pm 0.004
100% Real + 200% Synth	0.776 \pm 0.004	0.768 \pm 0.005

across all settings, with the advantage being more pronounced at lower real data fractions. This is because CFG explicitly conditions on labels, compensating for the minority class even when the unconditional model underrepresents rare events.

The lower half examines whether adding synthetic data to the full real dataset can improve performance. Unconditional augmentation at 100% and 200% achieves AUCs of 0.775 and 0.776, exceeding the baseline of 0.770, suggesting that diversity from synthetic data improves classifier generalization. However, performance declines with further augmentation, suggesting that excessive augmentation dilutes real data signals (see the supplementary material for detailed results across augmentation scales).

V. CONCLUSION

We proposed a continuous-time diffusion framework for generating mixed-type time-series electronic health records. By extending TabDiff with a BiGRU temporal backbone, unified Gaussian diffusion via continuous categorical embeddings, and factorized learnable noise schedules, our method achieves state-of-the-art performance on MIMIC-III and eICU datasets in downstream task utility, distribution fidelity, and discriminability, while requiring only 50 sampling steps compared to 1,000 for discrete-time baselines. The ablation study confirms that unified Gaussian diffusion is the primary contributor, and classifier-free guidance further enables effective conditional generation for data augmentation in class-imbalanced clinical scenarios.

Our method shows room for improvement in categorical marginal distribution fidelity and complex nonlinear inter-feature dependencies. Future work includes addressing these

limitations, validating on additional EHR datasets such as HiRID [35], and exploring applications to other temporal clinical data domains.

ACKNOWLEDGMENT

The authors would like to express their sincere gratitude to Prof. Dr. Prof. h.c. Andreas Dengel for his understanding and support in conducting this research.

REFERENCES

- [1] B. Shickel, P. J. Tighe, A. Bihorac, and P. Rashidi, "Deep ehr: a survey of recent advances in deep learning techniques for electronic health record (ehr) analysis," *IEEE journal of biomedical and health informatics*, vol. 22, no. 5, pp. 1589–1604, 2017.
- [2] K. Benitez and B. Malin, "Evaluating re-identification risks with respect to the hipaa privacy rule," *Journal of the American Medical Informatics Association*, vol. 17, no. 2, pp. 169–177, 2010.
- [3] J. M. Franklin, S. Schneeweiss, J. M. Polinski, and J. A. Rassen, "Plasmode simulation for the evaluation of pharmacoepidemiologic methods in complex healthcare databases," *Computational statistics & data analysis*, vol. 72, pp. 219–226, 2014.
- [4] J. Walonoski, M. Kramer, J. Nichols, A. Quina, C. Moesel, D. Hall, C. Duffett, K. Dube, T. Gallagher, and S. McLachlan, "Synthea: An approach, method, and software mechanism for generating synthetic patients and the synthetic electronic health care record," *Journal of the American Medical Informatics Association*, vol. 25, no. 3, pp. 230–238, 2018.
- [5] S. Biswal, S. Ghosh, J. Duke, B. Malin, W. Stewart, C. Xiao, and J. Sun, "Eva: Generating longitudinal electronic health records using conditional variational autoencoders," in *Machine learning for healthcare conference*. PMLR, 2021, pp. 260–282.
- [6] Y. Lee, Y. Chae, and K. Jung, "Leveraging vq-vae tokenization for autoregressive modeling of medical time series," *Artificial Intelligence in Medicine*, vol. 154, p. 102925, 2024.
- [7] E. Choi, S. Biswal, B. Malin, J. Duke, W. F. Stewart, and J. Sun, "Generating multi-label discrete patient records using generative adversarial networks," in *Machine learning for healthcare conference*. PMLR, 2017, pp. 286–305.
- [8] M. K. Baowaly, C.-C. Lin, C.-L. Liu, and K.-T. Chen, "Synthesizing electronic health records using improved generative adversarial networks," *Journal of the American Medical Informatics Association*, vol. 26, no. 3, pp. 228–241, 2019.
- [9] A. Torfi and E. A. Fox, "Corgan: Correlation-capturing convolutional generative adversarial networks for generating synthetic healthcare records," in *FLAIRS*, 2020, pp. 335–340.
- [10] J. Yoon, M. Mizrahi, N. F. Ghalaty, T. Jarvinen, A. S. Ravi, P. Brune, F. Kong, D. Anderson, G. Lee, A. Meir *et al.*, "Ehr-safe: generating high-fidelity and privacy-preserving synthetic electronic health records," *NPJ digital medicine*, vol. 6, no. 1, p. 141, 2023.
- [11] H. Karami, M.-A. Hartley, D. Aienza, and A. Ionescu, "Timehr: Image-based time series generation for electronic health records," *IEEE Journal of Biomedical and Health Informatics*, 2025.
- [12] J. Ho, A. Jain, and P. Abbeel, "Denoising diffusion probabilistic models," *Advances in neural information processing systems*, vol. 33, pp. 6840–6851, 2020.
- [13] Y. Song, J. Sohl-Dickstein, D. P. Kingma, A. Kumar, S. Ermon, and B. Poole, "Score-based generative modeling through stochastic differential equations," in *International Conference on Learning Representations (ICLR)*, 2021.
- [14] H. He, S. Zhao, Y. Xi, and J. C. Ho, "Meddiff: Generating electronic health records using accelerated denoising diffusion model," *arXiv preprint arXiv:2302.04355*, 2023.
- [15] T. Ceritli, G. O. Ghosheh, V. K. Chauhan, T. Zhu, A. P. Creagh, and D. A. Clifton, "Synthesizing mixed-type electronic health records using diffusion models," *arXiv preprint arXiv:2302.14679*, 2023.
- [16] A. A. Naseer, B. Walker, C. Landon, A. Ambrosy, M. Fudim, N. Wysham, B. Toro, S. Swaminathan, and T. Lyons, "ScoeHR: generating synthetic electronic health records using continuous-time diffusion models," in *Machine Learning for Healthcare Conference*. PMLR, 2023, pp. 489–508.
- [17] H. Yuan, S. Zhou, and S. Yu, "Ehrdiff: Exploring realistic ehr synthesis with diffusion models," *arXiv preprint arXiv:2303.05656*, 2023.
- [18] C. Lee, J. Kim, and N. Park, "Codi: Co-evolving contrastive diffusion models for mixed-type tabular synthesis," in *International Conference on Machine Learning*. PMLR, 2023, pp. 18940–18956.
- [19] J. Han, Z. Chen, Y. Li, Y. Kou, E. Halperin, R. E. Tillman, and Q. Gu, "Guided discrete diffusion for electronic health record generation," *Transactions on Machine Learning Research*, 2025. [Online]. Available: <https://openreview.net/forum?id=N2rWhTgits>
- [20] B. Deng, C. Xu, H. Li, Y.-h. Huang, M. Hou, and J. Bian, "Tardiff: Target-oriented diffusion guidance for synthetic electronic health record time series generation," in *Proceedings of the 31st ACM SIGKDD Conference on Knowledge Discovery and Data Mining V. 2*, 2025, pp. 474–485.
- [21] M. Tian, B. Chen, A. Guo, S. Jiang, and A. R. Zhang, "Reliable generation of privacy-preserving synthetic electronic health record time series via diffusion models," *Journal of the American Medical Informatics Association*, p. ocae229, 2024.
- [22] J. Shi, M. Xu, H. Hua, H. Zhang, S. Ermon, and J. Leskovec, "Tabdiff: a mixed-type diffusion model for tabular data generation," in *The Thirteenth International Conference on Learning Representations*, 2025. [Online]. Available: <https://openreview.net/forum?id=swvURjrt8z>
- [23] M. Mueller, K. Gruber, and D. Fok, "Continuous diffusion for mixed-type tabular data," in *The Thirteenth International Conference on Learning Representations*, 2025. [Online]. Available: <https://openreview.net/forum?id=QPtOBPN4IZ>
- [24] K. Cho, B. Van Merriënboer, C. Gulcehre, D. Bahdanau, F. Bougares, H. Schwenk, and Y. Bengio, "Learning phrase representations using rnn encoder-decoder for statistical machine translation," *arXiv preprint arXiv:1406.1078*, 2014.
- [25] A. Johnson, T. Pollard, and R. Mark, "MIMIC-III Clinical Database (version 1.4)," sep 2016. [Online]. Available: <https://doi.org/10.13026/C2XW26>
- [26] A. E. W. Johnson, T. J. Pollard, L. Shen, L.-w. H. Lehman, M. Feng, M. Ghassemi, B. Moody, P. Szolovits, L. A. Celi, and R. G. Mark, "MIMIC-III, a freely accessible critical care database," *Scientific Data*, vol. 3, p. 160035, 2016. [Online]. Available: <https://doi.org/10.1038/sdata.2016.35>
- [27] A. L. Goldberger, L. A. N. Amaral, L. Glass, J. M. Hausdorff, P. C. Ivanov, R. G. Mark, J. E. Mietus, G. B. Moody, C.-K. Peng, and H. E. Stanley, "PhysioBank, PhysioToolkit, and PhysioNet: Components of a new research resource for complex physiologic signals," *Circulation*, vol. 101, no. 23, pp. e215–e220, 2000. [Online]. Available: <https://www.ahajournals.org/doi/full/10.1161/01.CIR.101.23.e215>
- [28] T. J. Pollard, A. E. Johnson, J. D. Raffa, L. A. Celi, R. G. Mark, and O. Badawi, "The icu collaborative research database, a freely available multi-center database for critical care research," *Scientific data*, vol. 5, no. 1, pp. 1–13, 2018.
- [29] Y. Zhong, X. Wang, J. Wang, X. Zhang, Y. Wang, M. Huai, C. Xiao, and F. Ma, "Synthesizing multimodal electronic health records via predictive diffusion models," in *Proceedings of the 30th ACM SIGKDD Conference on Knowledge Discovery and Data Mining*, 2024, pp. 4607–4618.
- [30] H. He, Y. Xi, Y. Chen, B. Malin, J. Ho *et al.*, "A flexible generative model for heterogeneous tabular ehr with missing modality," in *The Twelfth International Conference on Learning Representations*, 2024.
- [31] S. Sahoo, M. Arriola, Y. Schiff, A. Gokaslan, E. Marroquin, J. Chiu, A. Rush, and V. Kuleshov, "Simple and effective masked diffusion language models," *Advances in Neural Information Processing Systems*, vol. 37, pp. 130 136–130 184, 2024.
- [32] T. Karras, M. Aittala, T. Aila, and S. Laine, "Elucidating the design space of diffusion-based generative models," *Advances in Neural Information Processing Systems*, vol. 35, pp. 26 565–26 577, 2022.
- [33] G. Bertasius, H. Wang, and L. Torresani, "Is space-time attention all you need for video understanding?" in *Icml*, vol. 2, no. 3, 2021, p. 4.
- [34] J. Ho and T. Salimans, "Classifier-free diffusion guidance," *arXiv preprint arXiv:2207.12598*, 2022.
- [35] S. L. Hyland, M. Faltys, M. Hüser, X. Lyu, T. Gumbsch, C. Esteban, C. Bock, M. Horn, M. Moor, B. Rieck *et al.*, "Early prediction of circulatory failure in the intensive care unit using machine learning," *Nature medicine*, vol. 26, no. 3, pp. 364–373, 2020.